



OPEN ACCESS

EDITED BY

Manas Sutradhar,
Lusofona University, Portugal

REVIEWED BY

Mauro Ravera,
Università del Piemonte Orientale, Italy
Nadiia I. Gumerova,
University of Vienna, Austria

*CORRESPONDENCE

Dinorah Gambino,
✉ dgambino@fq.edu.uy
Debbie C. Crans,
✉ debbie.crans@colostate.edu
Peter A. Lay,
✉ peter.lay@sydney.edu.au

RECEIVED 01 March 2024

ACCEPTED 05 June 2024

PUBLISHED 05 July 2024

CITATION

Levina A, Scalese G, Gambino D, Crans DC and Lay PA (2024), Solution chemistry and anti-proliferative activity against glioblastoma cells of a vanadium(V) complex with two bioactive ligands.
Front. Chem. Biol. 3:1394645.
doi: 10.3389/fchbi.2024.1394645

COPYRIGHT

© 2024 Levina, Scalese, Gambino, Crans and Lay. This is an open-access article distributed under the terms of the [Creative Commons Attribution License \(CC BY\)](https://creativecommons.org/licenses/by/4.0/). The use, distribution or reproduction in other forums is permitted, provided the original author(s) and the copyright owner(s) are credited and that the original publication in this journal is cited, in accordance with accepted academic practice. No use, distribution or reproduction is permitted which does not comply with these terms.

Solution chemistry and anti-proliferative activity against glioblastoma cells of a vanadium(V) complex with two bioactive ligands

Aviva Levina¹, Gonzalo Scalese^{2,3}, Dinorah Gambino^{2*},
Debbie C. Crans^{3*} and Peter A. Lay^{1*}

¹School of Chemistry, The University of Sydney, Sydney, NSW, Australia, ²Área Química Inorgánica, Facultad de Química, Universidad de la República, Montevideo, Uruguay, ³Department of Chemistry and Cell and Molecular Biology Program, Colorado State University, Fort Collins, CO, United States

Introduction: Glioblastoma is a brain cancer difficult to treat but recently mixed-ligand vanadium(V) Schiff base/catecholato complexes have exhibited high *in vitro* anti-proliferative activity. Hence, we explored the activity of $[V^{OL^1L^2}]$, which contains two iron chelating ligands, 2-hydroxy-1-naphthylaldehyde *iso*-nicotinoylhydrazone (L^1H_2) and clioquinol (L^2H). This complex was previously reported to be very effective against *Trypanosoma cruzi*, the causative agent of Chagas disease. These studies explored the possibility that a compound with efficacy against *Trypanosoma cruzi* also has efficacy against human glioblastoma cancer cells. Since $[V^{OL^1L^2}]$ was poorly soluble in water and the clioquinol ligand dissociated from the complex upon addition to an aqueous environment, an understanding of the speciation was very important to interpret its biological activity.

Methods: Stability studies in cell media were followed by UV/Vis spectroscopy to determine speciation of relevance to the *in vitro* anti-proliferative activity of the complex with T98G glioblastoma cells, which was also measured in the absence and presence of Fe(III).

Results and Discussion: The current work demonstrated that the mixed-ligand vanadium coordination complex had high *in vitro* anti-proliferative activity against the human glioblastoma (T98G) cell line. The enhanced anti-proliferative effects of the mixed-ligand vanadium complex against T98G cells could be due to either hydrolysis of complex and release of the toxic clioquinol, or the rapid uptake of the lipophilic complex prior to hydrolysis. The speciation studies showed that at least part of the potent toxicity of the mixed-ligand coordination complex stemmed from release of the bioactive clioquinol ligand from the complex, which depended on whether Fe(III) was present. The studies also showed that the $[V^V(O)_2(L^1H)]$ coordination complex was the most potent complex that remained intact and, hence, the complex that is the most biological active. Thus, future development of complexes should focus on the

one-ligand intact complexes or making any mixed-ligand complex more water soluble, stable in aqueous solution, or designed to be rapidly taken up by diseased cells prior to hydrolysis.

KEYWORDS

mixed-ligand vanadium complex, glioblastoma, enhanced anti-proliferative properties, speciation, complex hydrolysis, cellular uptake, albumin-V complex, Fe(III) chelating agent

1 Introduction

Vanadium is an element with biological significance, and numerous prospective therapeutic drugs based on vanadium have been proposed for addressing various diseases, particularly diabetes and cancer (Thompson et al., 2009; Levina and Lay, 2011; Willsky et al., 2011; Pessoa et al., 2015; Scior et al., 2016; Levina and Lay, 2017; Crans et al., 2019a; Pisano et al., 2019; Kowalski et al., 2020; Levina et al., 2020; Kostenkova et al., 2024). The applications of vanadium compounds for treatment of diabetes included clinical trials with vanadium salts and V(IV)-maltolato complex (BMOV) (Thompson et al., 2009; Levina and Lay, 2011; Willsky et al., 2011; Pessoa et al., 2015; Crans et al., 2019a; Kowalski et al., 2020). However, the number of applications of vanadium for treatment of diabetes significantly reduced the contributions in this area which was compounded when BMOV went of patent on 30 September 2011. For the past decade the interest in the application of vanadium compounds for treatment of cancer has dramatically increased. The vanadium coordination complexes used contain oxidovanadium(IV) and -(V) moieties including $V^{IV}O^{2+}$, $V^{VO}3^+$, $V^{VO}2^+$, and $V^{VO}3^-$ (Thompson et al., 2009; Willsky et al., 2011; Pessoa et al., 2015; Scior et al., 2016; Levina and Lay, 2017; Crans et al., 2019a; Pisano et al., 2019; Kowalski et al., 2020; Levina et al., 2020; Kostenkova et al., 2024). Additionally, polyoxometalates have also exhibited noteworthy biological activity (Bijelic et al., 2019; Aureliano et al., 2021; Kostenkova et al., 2023a). Different classes of cancers have been reported to be treated by vanadium compounds including *in vitro* efficacy against breast, prostatic, liver, kidney, bone, brain and other

cancers cell lines. Recent applications of vanadium compounds for treatment of cancers include applications of the next generation of cancer treatment such as oncolytic viruses that can be enhanced using vanadium compounds (Selman et al., 2018; Bergeron et al., 2019; McAusland et al., 2021). In addition, the potential for intratumoral application of vanadium compounds has recently been described, whereby high antiproliferative *in vitro* efficacy was demonstrated in cancer cell lines from difficult cancers to treat, such as the brain cancer, glioblastoma (Levina et al., 2020; Levina et al., 2022; Murakami et al., 2022; Kostenkova et al., 2023b; Levina et al., 2023). Glioblastoma is both difficult to treat and has very low survival rates once diagnosed.

Over the past 15–20 years rational design of vanadium-based compounds have been reported with the objective to develop agents against the parasite *Trypanosoma cruzi* (*T. cruzi*), causative agent of Chagas disease (Gambino, 2011; Pessoa et al., 2015; Scalese et al., 2015; Scalese et al., 2017; Scalese et al., 2018; Scalese et al., 2019; Mosquillo et al., 2020; Scalese et al., 2021; Scalese et al., 2022b). Chagas disease is an ancient endemic illness in Latin America considered a neglected disease (NTD) by the World Health Organization (Santos et al., 2020; WHO, 2023). Within this context, various series of $V^{IV}O^-$ and V^{VO} -based compounds were synthesized and demonstrated to have activity against *T. cruzi* (Gambino, 2011; Pessoa et al., 2015; Scalese et al., 2015; Scalese et al., 2017; Scalese et al., 2018; Scalese et al., 2019; Mosquillo et al., 2020; Scalese et al., 2021). Within these vanadium-based compounds, $[V^{VO}L^1L^2]$ (Figure 1), featuring L^1 as doubly deprotonated 2-hydroxy-1-naphthylaldehyde isonicotinoyl-hydrazone (Iron Chelator 311 or NIH, CAS 796-42-9) and L^2 as

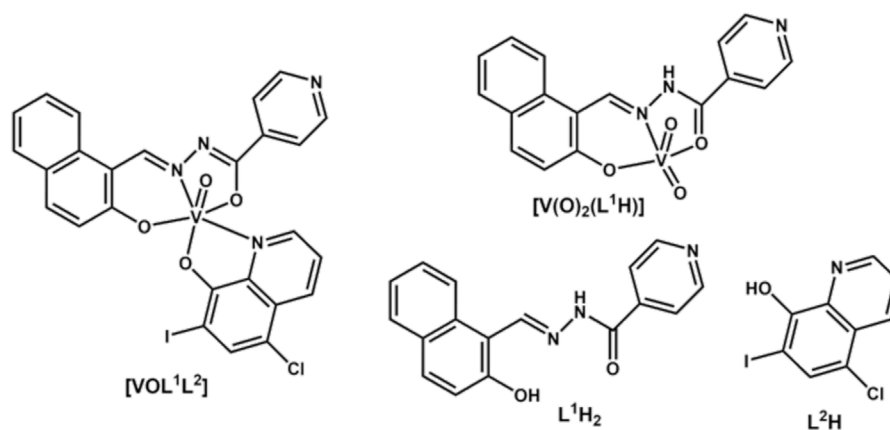


FIGURE 1
Structures of V(V) complexes and their ligands.

deprotonated 5-chloro-7-iodo-8-hydroxyquinoline (clioquinol, CAS 130-26-7), has been reported as a hit compound against *T. cruzi* (Scalese et al., 2021). $[V^{V}OL^1L^2]$ was selectively active against *T. cruzi* trypomastigotes, which is the infective form of the parasite found in the blood of infected humans, while being well tolerated by non-cancer mammalian (VERO) cells (Scalese et al., 2021).

The ligand L^1H_2 is a potent Fe(III) chelator that easily penetrates cell membranes (Buss et al., 2002) and shows anti-tubercular (Sah and Peoples, 1954; John et al., 2016), anti-malarial (Walcourt et al., 2004; Melnyk et al., 2006), anti-HIV (Debebe et al., 2007) and anti-cancer (Richardson et al., 1995; Green et al., 2001; Whitnall et al., 2006) activities. Clioquinol (L^2H_2) is a broad spectrum metal chelator with particularly strong affinity for Cu(II) and was widely used as an anti-protozoan drug but was withdrawn from clinical use due to neurotoxicity (Perez et al., 2019). However, it is currently still used for topical treatment of fungal infections (Prachayasittikul et al., 2013; Song et al., 2015; Oliveri and Vecchio, 2016; Chauhan et al., 2023). Investigations remain underway to develop safer and less toxic formulations of L^2H to harness its anti-microbial, anti-cancer and anti-neurodegenerative activities (Lanza et al., 2018; Khan et al., 2020; Joaquim et al., 2021; Chauhan et al., 2023). The approach of combining these two biologically active ligands, L^1H_2 and L^2H , with a biologically active metal ion, such as V(V), was explored and led to a complex with enhanced and selective anti-trypanosomal activity of $[V^{V}OL^1L^2]$ (Scalese et al., 2021). However, limited stability of V(V/IV) complexes in biological media and small therapeutic index are the main factors that prevented V-based drugs from entering clinical use in diabetes (Thompson et al., 2009; Scior et al., 2016). The former led to data misinterpretations in preclinical studies (Le et al., 2017; Levina and Lay, 2017; Nunes et al., 2021). In the case of $[V^{V}OL^1L^2]$, we found by ^{51}V NMR spectroscopy that the complex dissociates in aqueous solutions with the release of L^2H ligand and formation of the homoleptic complex, $[V^V(O)_2(L^1H)]$ (Figure 1) (Scalese et al., 2022a). As a result, we concluded that at least part of the observed efficacy and specificity on *T. cruzi* trypomastigotes cells are due to dissociated ligand (Scalese et al., 2021). However, binding of biologically active ligands to V(V/IV) ions can lead to improved activity via ligand stabilization and increased cellular uptake rate (Hamidi et al., 2016; Reytman et al., 2018; Murakami et al., 2022).

The potential for anti-cancer properties of the $[V^{V}OL^1L^2]$ complex were also postulated, since there are reported similarities in metabolism of protozoans such as *T. cruzi* and *Leishmania* and various human cancer cells (Martínez-Flórez et al., 2020; Dorosti et al., 2014; Perez et al., 2008). For example, some anti-trypanosomal compounds such as artemisinin and albendazole have demonstrated efficacy against experimental tumors and, conversely, antitumor agents such as imatinib, antifolates and cisplatin have displayed antiparasitic effects (Kinnamon et al., 1979; Perez et al., 2008; Dorosti et al., 2014; Scalese et al., 2017; Odularu et al., 2019; Rivas et al., 2019; Machado et al., 2023). Specifically, antigens such as Tn, TF, sial Tn and Tk have been found in both some parasites and in solid lymphoma tumors (Perez et al., 2008). However, this is of limited relevance to cancers of the brain since there is an additional requirement to traverse the blood-brain barrier (BBB). This not only requires drugs to be small and lipophilic (Wu et al., 2023),

but also for metal complex anti-cancer drugs to be sufficiently stable to traverse the BBB, which is not the case for $[V^{V}OL^1L^2]$ (Scalese et al., 2022a).

Despite these limitations, the differential reactivity of V(V/IV) complexes in cancer tumors and surrounding healthy tissues can be used to advantage in novel cancer treatments, particularly for brain and pancreatic cancers (Levina et al., 2020; Levina et al., 2022; Murakami et al., 2022; Kostenkova et al., 2024; Levina et al., 2023), where direct intratumoral injections have the potential to overcome the limitation of transport through the BBB (Levina et al., 2022). In particular, aggressive brain cancers are difficult to treat, with glioblastoma by far being the most common and aggressive form of glioma (brain tumor) with an average incidence of three cases per 100,000 individuals (Fakhoury, 2016). The difficulty in drug transport across the BBB, together with the high cell proliferation of glioblastoma and invasion with frequent recurrence after surgical intervention and chemotherapy presents a challenge for drug design (Fakhoury, 2016; Wu et al., 2023). Recent clinical trials and applications have looked to overcome some of these impediments by the use of intratumoral injections of highly cytotoxic or immunomodulating drugs. Next generation intratumoural injection approaches to treat glioblastoma currently in Phase I and II human clinical trials include those for platinum-based drugs (e.g., cisplatin and oxaliplatin), and T-Vec, which are drugs used to treat advanced melanoma and a range of other cancers (Hamid et al., 2020; Levina et al., 2022). Certain mixed Schiff base/catecholato and homoleptic catecholato complexes are amongst the few classes of V(V) species that have sufficient stability in cell culture media to be taken up by cancer cells intact to exert strong anti-proliferative activity against diverse cancer cell lines (Crans et al., 2019b; Griffin et al., 2019; Levina et al., 2020; Levina et al., 2022; Murakami et al., 2022; Kostenkova et al., 2023b; Levina et al., 2023). In this work, we explored detailed stability and anti-proliferative studies on $[V^{V}OL^1L^2]$ and $[V^V(O)_2(L^1H)]$ in a human brain cancer (glioblastoma) cell line, T98G, which was previously established as a lead model for anti-cancer activity studies of reactive V(V) complexes (Levina et al., 2020; Levina et al., 2022; Murakami et al., 2022; Kostenkova et al., 2023b). The speciation studies are crucial for understanding which species cause the biological activity of vanadium complexes with the objective to improve their design and ultimately promote their future clinical use (Scior et al., 2016; Levina et al., 2017; Levina and Lay, 2017; Crans et al., 2019a; Levina et al., 2023).

2 Materials and methods

2.1 General materials and methods

Common laboratory chemicals and the L^2H free ligand (analytical grade, >99% purity) from Merck were used without additional purification, and water was purified by the MilliQ technique. The following sources of proteins (Merck) were used: human apo-transferrin (Tf; >98% protein; $\leq 0.005\%$ Fe; Cat. No. T1147), and human serum albumin (HSA; >99% protein; Cat.

No. A8763). The ligand L^1H_2 and the V(V) complexes, $[VOL^1L^2]$ and $[V(O)_2(L^1H)]$, were synthesized and characterized previously in the Gambino group (Scalese et al., 2021). Stock solutions of complexes or free ligands in dimethyl sulfoxide (DMSO) or dimethylformamide (DMF) were prepared on the day of experiments. Solutions in DMF were used for mass spectrometry only, due to the detrimental effect of DMSO in this technique. Stock solutions of Fe(III)-citrate (~10 mM) were prepared by mixing aqueous solutions of $Fe(NO_3)_3 \cdot 9H_2O$ and citric acid disodium salt (1:2 metal to ligand molar ratio), and adjusting the pH value to ~5.0 with aqueous NaOH (1.0 M). Precise Fe(III) concentrations in these solutions were determined by graphite furnace AAS, using an Agilent Technologies Series 200 spectrometer (equipped with Zeeman background correction) and certified Fe(III) standard (Aldrich Cat. No. 16596). Stock solutions of sodium ascorbate (0.50 M) were prepared immediately before use by dissolving solid ascorbic acid (Merck 255564) in 0.50 M aqueous NaOH.

Stabilities of V(V) complexes and ligands were studied by electronic absorption (UV-vis-NIR) spectroscopy at 310 K in either phosphate buffered saline (PBS, containing 150 mM NaCl and 20 mM phosphate buffer, pH 7.4) or in cell culture medium without phenol red (Thermo Fisher Scientific, Cat. No. 31053-028, CCM) that was fully supplemented according to the conditions of cell assays (see below), and additionally supplemented with 2-[4-(2-hydroxyethyl)piperazin-1-yl]ethanesulfonic acid (HEPES, 10 mM) to maintain pH 7.4 under ambient atmosphere (Levina et al., 2017). The pH values of PBS and media were checked immediately before use with Activon 210 ionometer that was equipped with AEP 321 glass/Ag/AgCl electrode and calibrated daily using standard pH solutions (Aldrich). The UV-vis-NIR spectra were acquired over the 300–1,020 nm range (resolution, 0.5 nm) on a Specord S600 diode-array spectrometer (Analytic Jena, Germany) that was equipped with a HP89090A Peltier temperature controller.

Low-resolution electrospray ionization mass spectrometry (ESI-MS) data for complexes and free ligands were collected on a Bruker amaZon SL spectrometer, using the following parameters: nebulizer pressure, 27.3 psi; spray voltage, 4.5 kV; capillary temperature, 453 K; N_2 flow rate, 4 L min^{-1} ; m/z range, 100–1,000 (alternating positive- and negative-ion modes). Analyzed solutions (5.0 μL) were injected into a flow of MeOH (flow rate, 0.30 mL min^{-1}). Acquired spectra were the averages of 100–200 scans (scan time, 10 ms). Solutions for mass spectrometry were prepared by diluting stock solutions of V(V) complexes or the ligands (10 mM in DMF) 200-fold either with pure MeOH, or with MeOH/ H_2O mixture (1:1 vol/vol) that contained NH_4HCO_3 (10 mM, pH 7.5) (Le et al., 2017; Griffin et al., 2019). Simulations of the mass spectra were performed using IsoPro software (version 3.0, M. Senko, Sunnyvale, CA, United States, 1998).

Concentrations of V in cell digests were determined by ICP-MS with a Perkin-Elmer Nexion 350X spectrometer, using a standard V(IV) solution (Choice Analytical, Australia) and ^{193}Ir the peak as an internal standard. The measurements were performed in kinetic energy discrimination (KED) mode to eliminate the interference of $[^{35}Cl^{16}O]^+$ ions with the determination of $^{51}V^+$ (Sarmiento-Gonzalez et al., 2005).

2.2 Cell culture, proliferation and V uptake assays

Pre-sterilized media and sterile plasticware used in cell culture were purchased from Thermo Fisher Scientific Australia. The well-established human cancer cell lines: T98G (glioblastoma multiforme, CRL-1690) and HFF-1 (normal human foreskin fibroblasts, SCRC-1041) were purchased from the American Type Culture Collection (ATCC) and used at passages four to six. The cells were cultured using standard techniques (Freshney, 2016) in Advanced DMEM (Cat. No. 12491-015), supplemented with L-glutamine (2.0 mM), antibiotic-antimycotic mixture (100 U mL^{-1} penicillin, 100 mg mL^{-1} streptomycin and 0.25 mg mL^{-1} amphotericin B) and fetal calf serum (FCS; heat-inactivated; 2% vol). For proliferation experiments, cells were seeded in 96-well plates at an initial density of 1.0×10^3 (T98G) or 3.0×10^3 (HFF-1) viable cells per well in 100 μL medium and left to attach overnight.

Cell proliferation was measured in 72 h assays using either fully supplemented growth medium or the medium additionally supplemented with physiological concentration of human serum albumin (HSA, 0.60 mM), human apo-transferrin (Tf, 30 μM) (Levina et al., 2023) or sodium ascorbate (5.0 mM). These additionally supplemented media were prepared immediately before use and filtered through a sterile 0.22 μm pore membrane (Merck SLGP044RS). Stock solutions of $[VOL^1L^2]$, $[V(O)_2(L^1H)]$, L^1H_2 or L^2H (10 mM in DMSO) were serially diluted two-fold with DMSO and then added to cell culture media so that all the treatments, including controls, contained 1.0% (vol.) DMSO, which was well tolerated by the cells (Ilieva et al., 2021). Stock solutions of Fe(III)-citrate and Na_3VO_4 (10 mM in H_2O) were serially diluted with sterile water. Cell culture media containing the treatment compounds at the required final concentrations were either added to the cells within 1 min (fresh solutions) or left in cell culture incubator (310 K, 5% CO_2) for 24 h prior to the cell treatments (aged solutions) (Griffin et al., 2019; Levina et al., 2020; Murakami et al., 2022; Kostenkova et al., 2023b; Levina et al., 2023). Each treatment included six replicate wells and two background wells that contained the same components except the cells. After 72 h incubation with the treatment compound, the treatment medium was removed and the medium containing MTT reagent (1-(4,5-dimethylthiazol-2-yl)-3,5-diphenylformazan, Sigma M5655; 1.0 mg mL^{-1} ; prepared immediately before use) (Sylvester, 2011) was added. After 4–6 h incubation with MTT reagent, the medium was removed, the blue formazan crystals were dissolved in 0.10 mL per well of DMSO, and the absorbance at 600 nm was measured using Victor V3 plate reader. Typically, the treatment compounds were applied in a series of nine two-fold dilutions, starting from 100 μM V, plus the DMSO control, and the IC_{50} values were calculated using Origin Pro software (2022 version, OriginLab, Northampton, MA, United States). Note that $[VOL^1L^2]$ partially precipitated at the highest concentration, while all the other compounds were fully soluble in the medium up to 100 μM .

For V uptake experiments, T98G cells were grown to ~80% confluence in twelve-well plates (three replicas per treatment). Incubations with the treatment compounds (50 μM V; freshly

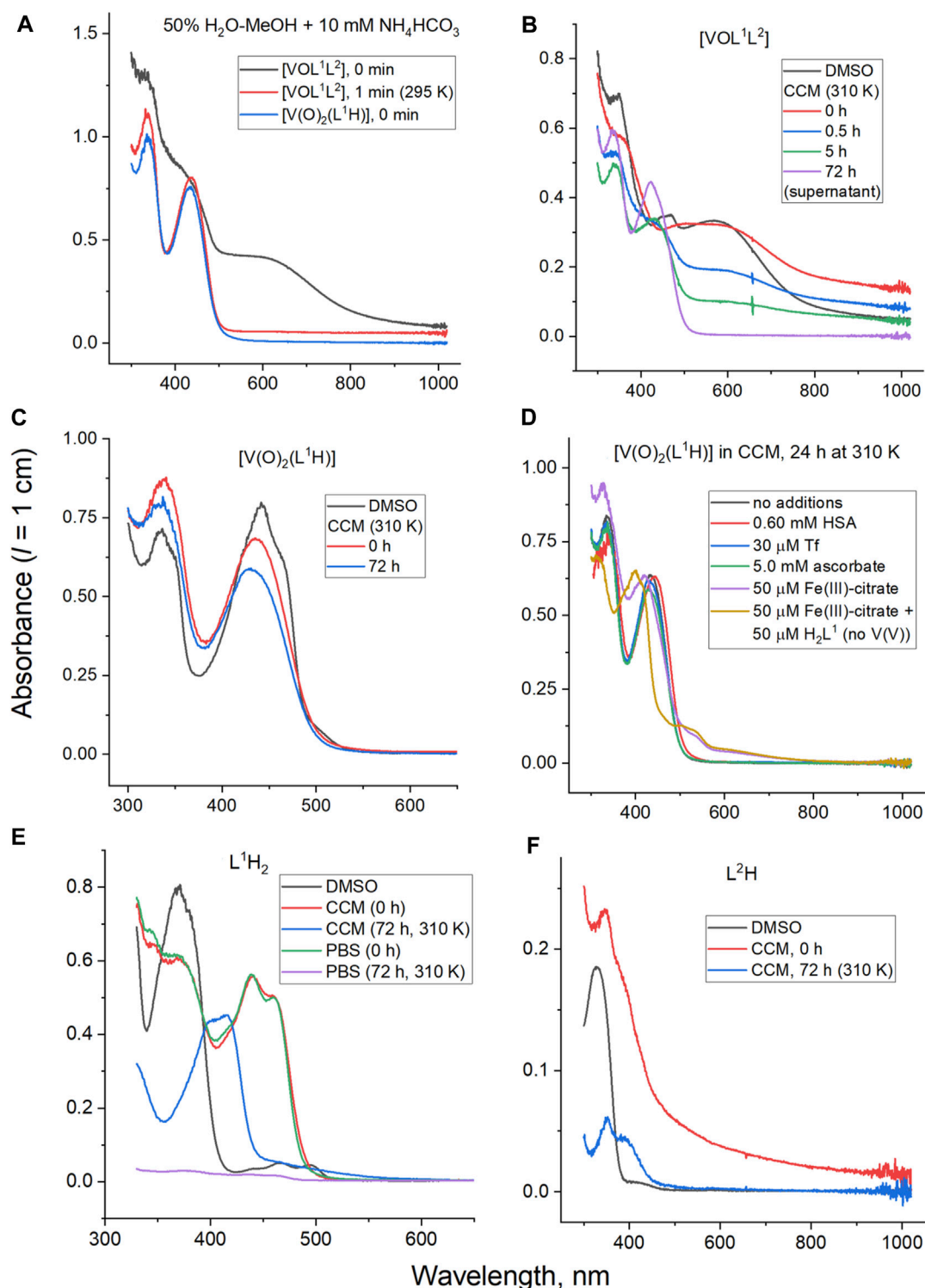


FIGURE 2 Typical UV-vis-NIR spectra of V(V) complexes, their free ligands and decomposition products at 50 μM concentration: **(A)** decomposition of $[\text{VOL}^1\text{L}^2]$ under the conditions matching those of ESI-MS studies; **(B)** decomposition of $[\text{VOL}^1\text{L}^2]$ under the conditions matching those of cell assays (CCM is cell culture medium, see Materials and Methods for details); **(C)** decomposition of $[\text{V}(\text{O})_2(\text{L}^1\text{H})]$ under the conditions matching those of cell assays; **(D)** decomposition of $[\text{V}(\text{O})_2\text{H}^1]$ under cell assay conditions in the presence of serum proteins, ascorbate or Fe(III); **(E)** comparison of decomposition products of L^1H_2 in CCM and phosphate buffered saline (PBS); and **(F)** decomposition of L^2H in CCM.

added to fully supplemented medium) were performed for 1 h at 310 K, 5% CO_2 . Longer treatments were not used due to high toxicity of some of the compounds, which led to premature cell

detachment. After the treatments, V-containing media were removed, the cell layers were washed twice with PBS, detached with TrypLE solution, pelleted, and washed again with PBS.

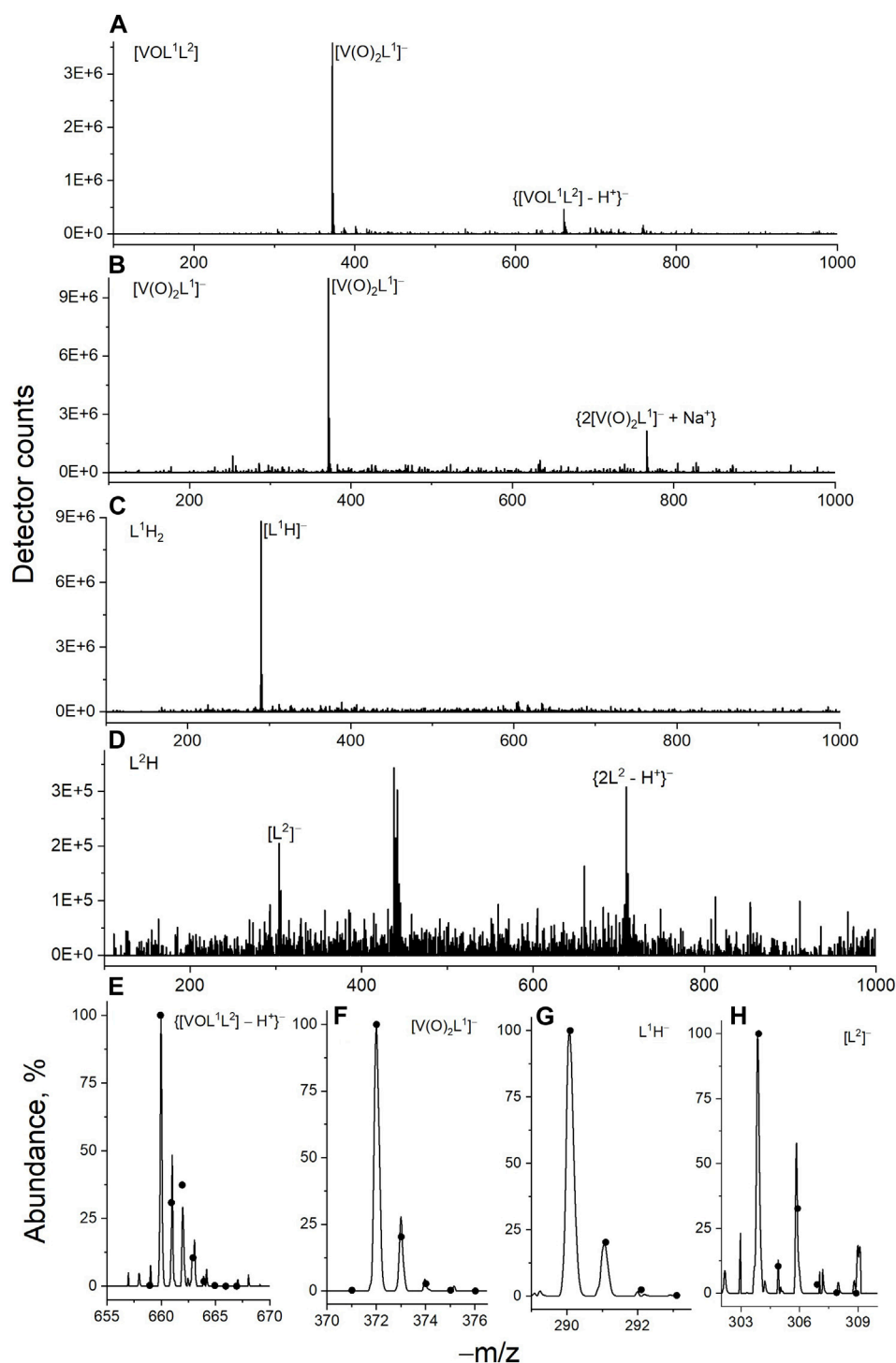


FIGURE 3

Typical ESI-MS data for V(V) complexes and their free ligands (50 μ M in 50% MeOH-H₂O containing 10 mM NH₄HCO₃; negative-ion mode) taken immediately after preparation: (A) $[VOL^1L^2]^-$; (B) $[V(O)_2(L^1H)]^-$; (C) L^1H_2 ; (D) L^2H ; (E-H) experimental (lines) and fitted (dots, calculated with IsoPro software) signals of main species.

Detachment and washing of cell pellets were used to remove V that was absorbed on the culture plates and on the cell surface (Jensen et al., 2011). Cell numbers in each pellet were counted with Countess automatic counter, typical numbers were $(2 \pm 0.5) \times 10^5$ cells/well, cell viability was >95% (Trypan blue

staining). Cell pellets were digested with 0.20 mL of 65% HNO₃ (trace pure, Fluka Cat. No. 30709) for 3 days at 295 K, then diluted with Milli-Q water to 1.0 mL for ICP-MS analysis. Cellular V concentrations were expressed in atoms V per cell.

3 Results

3.1 Reactivities of V(V) complexes and their ligands under the conditions of T98G cell assays

Decomposition of V(V) complexes under the conditions matching those of cell viability assays was studied using a combination of electronic absorption (UV-vis-NIR) and electrospray mass spectrometry (ESI-MS) techniques (Le et al., 2017; Griffin et al., 2019; Levina et al., 2023). A water-methanol mixture (H₂O: MeOH = 1 : 1 v/v) containing a volatile buffer (10 mM NH₄HCO₃, pH ~ 7.5) was used as an approximation for biological conditions that were compatible with the ESI-MS studies (Le et al., 2017; Griffin et al., 2019; Levina et al., 2023). When freshly prepared stock solution of [VOL¹L²] (10 mM, dark blue) in dimethyl sulfoxide (DMSO) was diluted 200-fold with the H₂O-MeOH-NH₄HCO₃ mixture, the initial blue color (shoulder at ~600 nm; black line in Figure 2A) disappeared within ~1 min at 295 K, which led to a yellow solution (maxima at 335 and 435 nm; red line in Figure 2A). This spectrum closely matched that of the corresponding dilution of [V(O)₂(L¹H)] (final V concentration, 50 μM; blue line in Figure 2A). A slight increase in background absorbance in red vs. blue line in Figure 2A was likely due to the light scattering by colloidal particles formed by the poor water-solubility of L²H (Cayman Chemicals, 2023). Rapid decomposition of [VOL¹L²] (50 μM) in H₂O-MeOH-NH₄HCO₃ solution with the formation of [V(O)₂(L¹H)] was confirmed by ESI-MS (negative ion mode; *m/z* = 372 for the deprotonated form, [V(O)₂L¹]⁻), while traces of the original complex were observed at *m/z* = 660 (Figure 3A). In agreement with the previous results of ⁵¹V NMR studies (Scalese et al., 2022a), these data indicated that [VOL¹L²] rapidly decomposed in aqueous media with the release of 8-hydroxyquinoline ligand (L²H) and formation of the homoleptic complex [V(O)₂(L¹H)]. The ESI-MS data (negative ion mode) of 50 μM solutions of [V(O)₂(L¹H)], L¹H₂ or L²H in H₂O-MeOH-NH₄HCO₃ showed the signals due to [V(O)₂L¹]⁻ (*m/z* = 372), [L¹H]⁻ (*m/z* = 290) and [L²]⁻ (*m/z* = 305), respectively, although the latter signal was poorly defined due to the low water solubility of L²H (Figures 3B–D). The corresponding experimental and calculated isotopic distributions are shown in Figures 3E–H.

Time-dependent UV-vis-NIR spectral changes during the decomposition of [VOL¹L²] under the conditions that closely matched those of cell culture assays (50 μM V, fully supplemented cell culture medium, pH 7.4, 310 K) (Levina et al., 2017) are shown in Figure 2B. The initial spectrum of [VOL¹L²] in cell culture medium (CCM; red line in Figure 2B) showed a broad absorbance band at ~600 nm, which resembled that of a 50 μM [VOL¹L²] solution in DMSO (black line in Figure 2B), except for an elevated absorbance background due to the formation of colloidal particles. The ~600 nm band gradually disappeared within ~10 h to give rise to the characteristic absorbance bands of [V(O)₂(L¹H)] at 335 and 345 nm (blue and green lines in Figure 2B), which was also confirmed by ESI-MS data (Figure 3A) and the published ⁵¹V NMR data (Scalese et al., 2022a). After 72 h incubation at 310 K and centrifugation to remove insoluble particles (2 min at 16,000 g), the spectrum of the supernatant was consistent with a ~40 μM [V(O)₂(L¹H)] solution (purple line in Figure 2B). The remaining

blue precipitate was fully soluble in DMSO and showed the spectrum consistent with that of [VOL¹L²]. Taken together, the data contained within Figures 2A, B indicated that [VOL¹L²] (50 μM) gradually dissolved in CCM on the hours timescale at 310 K, while the dissolved fraction rapidly converted to [V(O)₂(L¹H)]. This gradual dissolution explained the apparently slower decomposition of [VOL¹L²] in CCM (an entirely aqueous medium; Figure 2B) compared with 50% H₂O-MeOH solution that completely dissolved [VOL¹L²] at this concentration (Figure 2A).

Unlike for [VOL¹L²], the homoleptic [V(O)₂(L¹H)] complex was fully soluble at 50 μM and highly stable in CCM, showing ~10% decrease in absorbance at 335 and 345 nm after 72 h incubation at 310 K (red and blue lines in Figure 2C). The spectra of [V(O)₂(L¹H)] in CCM were also close to that in DMSO solution (black line in Figure 2C). No significant changes in the spectra of [V(O)₂(L¹H)] were observed after 24 h of incubation (310 K) in CCM that contained physiologically relevant concentrations of two main metal-binding proteins human serum albumin (0.60 mM), or transferrin (30 μM) (Ritchie et al., 2002; Levina et al., 2020; Levina and Lay, 2020; Levina et al., 2023) (black, red and blue lines in Figure 2D). Similarly, no changes occurred in the presence of 100-fold molar excess of a strong biological reductant, ascorbate (green line in Figure 2D). Other V(V) complexes are known to be rapidly reduced to V(IV) species by ascorbate in neutral aqueous solutions (Wilkins et al., 2006; Horton et al., 2014). By contrast, significant spectral changes, including the formation of two new broad absorbance bands at 500–700 nm, were observed during the reaction of 50 μM [V(O)₂(L¹H)] with an equimolar amount of Fe(III)-citrate in CCM for 24 h at 310 K (purple line in Figure 2D). A similar spectrum was observed following the reaction of L¹H₂ with Fe(III)-citrate under the same conditions (yellow line in Figure 2D). These results show that Fe(III) can successfully compete with V(V) for the binding to L¹H₂ (a known strong Fe(III) chelator) (Buss et al., 2003; Whitnall et al., 2006; Debebe et al., 2007; Kalinowski et al., 2008) under physiologically relevant conditions. A similar reaction in cell culture medium led to a new absorbance band at ~410 nm (Figure 2E) due to the likely formation of new Schiff base product (Levina et al., 2023).

An immediate shift of the main absorbance band from 370 nm to 440 nm was observed when L¹H₂ (50 μM) was dissolved in CCM compared with the corresponding solution in DMSO (black and red lines in Figure 2E), which corresponded to a color change from pale to bright yellow. This change was due to deprotonation of L¹H₂ and tautomeric equilibrium in the L¹H⁻ anion, which led to the formation of conjugated double bonds [reaction (1) in Scheme 1]. Another spectral change occurred within 24 h of incubation of L¹H₂ with CCM at 310 K, which led to a single absorbance maximum at 415 nm (the spectrum at 72 h incubation, which was not significantly different from that at 24 h, is shown with a blue line in Figure 2E). The initial spectrum of L¹H₂ in PBS was nearly identical to that in CCM (green and red lines in Figure 2E), but the absorbance at >300 nm practically disappeared after 72 h incubation at 310 K (purple line in Figure 2E). This change is consistent with the hydrolysis of L¹H₂ to aldehyde and hydrazine precursors [reaction (2) in Scheme 1] (Buss and Ponka, 2003). The different spectra of reaction products in PBS and CCM point to the likely further reactions with CCM components, such as amine groups of amino acids and aldehyde groups of sugars (Levina et al., 2017), with the formation of Schiff base products [reaction (3) in

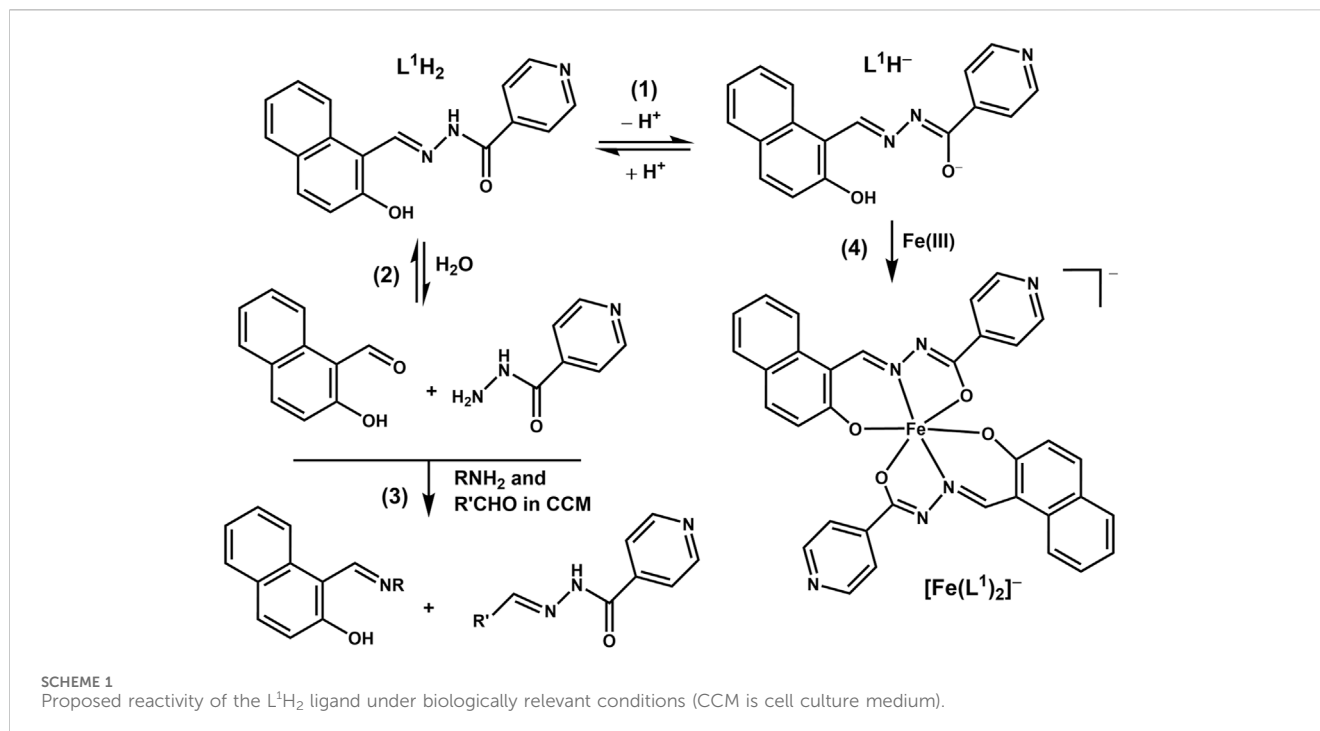


TABLE 1 Anti-proliferative activities of V(V) complexes and their ligands in T98G (human glioblastoma) and HFF-1 (normal human skin fibroblast) cell lines.

Compound	IC ₅₀ , μM (T98G) ^a	IC ₅₀ , μM (HFF-1) ^a	Uptake (T98G) ^b
[VOL ¹ L ²]	6.4 ± 0.4 (7.8 ± 0.6) ^c	36 ± 5	ND ^d
[V(O) ₂ (L ¹ H)]	3.1 ± 0.2 (3.9 ± 0.4) ^c	16 ± 2	23 ± 7
[V(O) ₂ (L ¹ H)] + HSA ^e	>100	ND ^d	19 ± 13
[V(O) ₂ (L ¹ H)] + Tf ^e	~0.2	ND ^d	21 ± 4
[V(O) ₂ (L ¹ H)] + HSA + Tf ^e	>100	ND ^d	13 ± 8
[V(O) ₂ (L ¹ H)] + ascorbate ^f	69 ± 8	ND ^d	25 ± 7
[V(O) ₂ (L ¹ H)] + Fe(III) ^g	63 ± 5	ND ^d	35 ± 8*
L ¹ H ₂	1.7 ± 0.1 (3.7 ± 0.3) ^c	12 ± 3	—
L ¹ H + Tf ^e	~0.2	ND ^d	—
L ¹ H + HSA ^e	~100	ND ^d	—
L ¹ H ₂ + Fe(III) ^g	76 ± 8	ND ^d	—
L ² H ₂	4.9 ± 0.5 (4.5 ± 0.6) ^c	24 ± 3	—
Na ₃ VO ₄	26 ± 4 ^h (24 ± 4) ^{c,h}	23 ± 3 ^h	75 ± 21*

^aConcentrations of the compounds that caused 50% decrease in cell viability in 72 h assays. Typical concentration-viability curves are shown in Figure 4. Unless noted otherwise, dilutions of the compounds (0–100 μM) in cell culture medium were added to the cells within 1 min after the preparation. Values are the means and standard deviations of six replicate wells.

^bVanadium uptake (million V atoms per cell) after 1 h treatment of T98G cells with 50 μM V complexes; mean values and standard deviations for three replicate wells. Values designated with asterisks are significantly ($p < 0.05$) higher than the value for [V(O)₂(L¹H)].

^cDilutions of the compounds (0–100 μM) in cell culture medium were pre-incubated at 310 K and 5% CO₂ for 24 h, then added to the cells for further 72 h.

^dValues not determined.

^ePhysiological concentrations (Ritchie et al., 2002) of HSA (0.60 mM) and/or Tf (30 μM) were added to cell culture medium. Addition of HSA, also provides close to physiological concentrations of Fe(III) (10–15 μM) (Levina and Lay, 2020).

^fTreatments with [V(O)₂(L¹H)] (0–100 μM) in the presence of excess ascorbate (5.0 mM).

^gTreatments with [V(O)₂(L¹H)] or L¹H₂ (0–100 μM) in the presence of equimolar amounts of Fe(III)-citrate.

^hData from (Murakami et al., 2022).

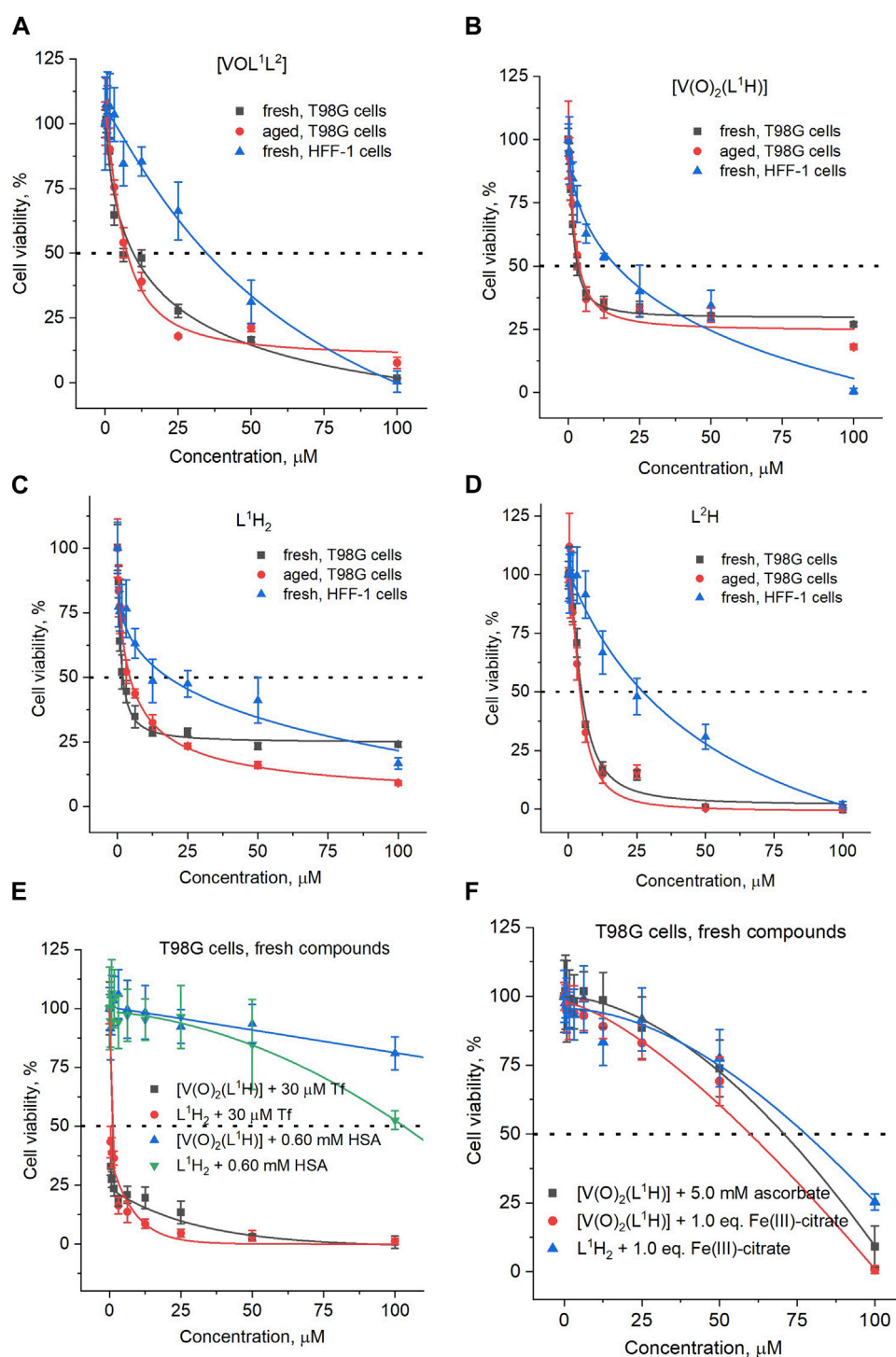


FIGURE 4

Typical concentration-viability dependencies of (A) [VOL¹L²] treatments of T98G or HFF-1 cells; (B) [V(O)₂(L¹H)] treatments of T98G or HFF-1 cells; (C) L¹H₂ treatments of T98G or HFF-1 cells; (D) L²H treatments of T98G or HFF-1 cells; (E) treatments of T98G cells with fresh solutions [V(O)₂(L¹H)] in the presence of serum proteins (HSA is human serum albumin and Tf is human apo-transferrin); (F) treatments of T98G cells with fresh solutions [V(O)₂(L¹H)] or L¹H₂ in the presence of excess ascorbate or equimolar concentrations of Fe(III). Fresh solutions: final dilutions of treatment compounds in CCM were added to cells within 1 min; aged solutions: final dilutions of treatment compounds in CCM were pre-incubated at 310 K and 5% CO₂ for 24 h before addition to cells. The corresponding IC₅₀ values are listed in Table 1. Dots and error bars represent median values and standard deviations of six replicate wells.

Scheme 1]. These reactions are consistent with the previous observations (Buss and Ponka, 2003) of L¹H₂ hydrolysis being faster in CCM compared with simple aqueous buffers. In addition, the intact ligand can bind Fe(III) and other trace metals in the medium [reaction (4) in Scheme 1 shows the example of Fe(III) binding] (Richardson and Bernhardt, 1999).

In contrast to the spectrum of 50 μM L²H in DMSO that showed a single sharp absorbance band at 330 nm (black line in Figure 2F), the corresponding spectrum in CCM showed a broad absorbance across the entire visible range (red line in Figure 2F), possibly due to non-covalent association with hydrophobic components of CCM, particularly serum proteins (Levina et al., 2017). This absorbance largely disappeared after 72 h incubation (blue line in Figure 2F), and is likely due to precipitation of poorly soluble L²H (Cayman Chemicals, 2023). A weak new absorbance band at ~400 nm was likely due to complexation of L²H to trace transition metal ions in the medium as reported previously (Lanza et al., 2018; Lopez et al., 2019).

3.2 Effect of reactivity on the anti-proliferative activities of V(V) complexes and their ligands in cultured human cells

A comparison of IC₅₀ values for the anti-proliferative activities of [VOL¹L²], [V(O)₂(L¹H)] and their free ligands (L¹H₂ and L²H) in human glioblastoma (T98G) cells and non-cancer skin fibroblasts (HFF-1) is given in Table 1, and the corresponding concentration-viability curves are shown in Figure 4. Similarly high activities (IC₅₀ < 10 μM) were observed for all four compounds in T98G cells; this included both fresh and aged (24 h at 310 K) solutions (Table 1). The activities of all four compounds in HFF-1 cells showed favorable selectivity with 5-6-fold higher IC₅₀ values than for T98G cells (Table 1). The cytotoxic activities of [V(O)₂(L¹H)] and L¹H for T98G cells were both an order of magnitude better than vanadate (Na₃VO₄). In addition, their selectivities were superior since vanadate cytotoxicities were the same for the two cell lines (Table 1) (Murakami et al., 2022). The concentration-viability profiles for all the compounds did not follow the classical sigmoidal shape (Sylvester, 2011) and showed a sharp decrease in viability at 0–10 μM, followed by a slower decrease at 10–100 μM (Figures 4A–D).

Unlike for the previously studied V(V)-Schiff base catecholato complexes (Crans, et al., 2019b, et al., 2023c; Levina et al., 2020; Murakami et al., 2022; Levina et al., 2023), the mixed-ligand complex, [VOL¹L²], was ~2-fold less active than [V(O)₂(L¹H)], in both cell lines studied (Table 1), which can be attributed to the slow dissolution of [VOL¹L²] under cell culture conditions (Figure 2A). Given the rapid conversion of dissolved [VOL¹L²] into [V(O)₂(L¹H)] and L²H (Figures 2A,B), the latter two compounds were likely responsible for the anti-proliferative activity of [VOL¹L²], but their activity was not synergistic, which is consistent with similar activities of fresh and aged solutions of [VOL¹L²] (Table 1). The activities of fresh and aged solutions of [V(O)₂(L¹H)] were also similar (Table 1), which is consistent with its high stability in CCM (Figure 2C). Similar activities were also observed for fresh and aged solutions of L²H (Table 1), despite its low water solubility and gradual precipitation in CCM (Figure 2F),

which indicates that the activity was due to the soluble fraction of the ligand. Remarkably, L¹H₂ retained significant activity in aged solutions (Table 1), despite its known decomposition into aldehyde and hydrazine precursors [reaction (2) in Scheme 1] (Buss and Ponka, 2003). This activity can be explained by the reactions of the formed precursors with CCM components that can lead to new bioactive molecules, as indicated by the differences in the UV-vis-NIR spectra of decomposition products of L¹H₂ in CCM and PBS solutions (Figure 2E).

Despite the absence of obvious changes in the UV-vis-NIR spectra of [V(O)₂(L¹H)] in the presence of physiological concentrations (Ritchie et al., 2002) of HSA and apoTf (0.60 mM and 30 μM, respectively, Figure 2D), these proteins had profound and opposite effects on the anti-proliferative activity of the complex in T98G cells (Table 1; Figure 4E). The presence of HSA abolished the activity of [V(O)₂(L¹H)], while Tf drastically increased it (black and blue lines in Figure 4E). A mixture of physiological concentrations of HSA and Tf reduced the activity [V(O)₂(L¹H)], similarly to the effect of HSA alone (Table 1, not shown in Figure 4E). These effects were in stark contrast with those observed for inorganic V salts, Na₃VO₄ and VOSO₄, where Tf alone or in combination with HSA reduced the activity, while HSA alone slightly increased it (Levina and Lay, 2020). Remarkably, the effect of Tf and HSA on the activity [V(O)₂(L¹H)] was mirrored by that for the free ligand, L¹H₂ (Table 1 and red and green lines in Figure 4E).

As shown in Table 1 and Figure 2F (red and blue lines), the anti-proliferative activities of [V(O)₂(L¹H)] and L¹H₂ decreased 20-40-fold in the presence of equimolar concentrations of Fe(III)-citrate, due to the binding of Fe(III) to L¹H₂ (reaction (4) in Scheme 1) and displacement of V(V) from [V(O)₂(L¹H)] (Figure 2D). Therefore, the decrease in viability of T98G cells by ~70% in the presence of the lowest used concentrations [V(O)₂(L¹H)] or L¹H₂ (0.39 μM) and 30 μM Tf (black and red lines in Figure 2E) was likely due to the binding by Tf of the trace Fe present in the medium (typically, 1–2 μM) (Levina and Lay, 2020). The inhibitory effect of HSA on the activities of [V(O)₂(L¹H)] or L¹H₂ is harder to explain at this stage, but it may be due to the blockage of cellular uptake of the compounds by their non-covalent transient binding to HSA (Levina et al., 2023). Physiologically relevant concentration of ascorbate (5.0 mM) (Przybyło and Langner, 2020) also reduced the activity of [V(O)₂(L¹H)] (Table 1) despite the stability of the complex to reduction by ascorbate (Figure 2D). This can be due to the general protective effect of ascorbate against the toxicity of [V(O)₂(L¹H)] that is likely to involve generation of reactive oxygen species (Horton et al., 2014; Aureliano et al., 2023).

Uptake of V from [V(O)₂(L¹H)] (50 μM for 1 h at 310 K) by T98G cells was low (on the order of 10⁷ V atoms per cell) (Levina et al., 2023) and did not exceed that from Na₃VO₄ (Table 1), which was consistent with the previous results for [V(O)₂L] complexes, where L is a deprotonated Schiff base (Murakami et al., 2022; Kostenkova et al., 2023b). Notably, cellular V uptake from [V(O)₂(L¹H)] slightly but significantly increased in the presence of an equimolar amount of Fe(III)-citrate, which suggests that V(V) ions that are displaced from [V(O)₂(L¹H)] by Fe(III)-citrate (Figure 2D) can enter cells more efficiently than the intact complex.

4 Discussion

This work was undertaken to evaluate the potential medicinal applications of the mixed-ligand complex, $[VOL^1L^2]$ (Scalese et al., 2021), for potential treatment of glioblastoma (T98G cells), where the both ligands are known chelators of essential metal ions (Fe(III) and Cu(II)). The utility of the mixed-ligand complex was complicated by its poor water solubility and the rapid decomposition in aqueous medium. However, it was the objective to investigate the activity of any potential decomposition products upon hydrolysis of the complex. To our surprise, the two main decomposition products, $[V(O)_2(L^1H)]$ and L^2H , were found to be more active than the intact complex against glioblastoma (Table 1). Considering the stability in aqueous medium (Figure 2D) and biological activity (Table 1) of the precursor $[V(O)_2(L^1H)]$ complex, it may be the most promising potential future agent against cancer, unless future mixed complexes are significantly more soluble and have increased stability. This result was unexpected, and only was discovered by the speciation studies, which emphasized the importance of considering the chemistry of these complexes in a biological environment. Although it should be noted that our speciation studies, despite our attempts to replicate physiologically relevant conditions, will not exactly mimic the cellular environment. Since the complex does decompose it seems clear that in the reported studies with the mixed-ligand vanadium complex in *T. cruzi* the observed activity is a combination of the vanadium complex and that of free ligand (Scalese et al., 2021), and that the free clioquinol is likely responsible for the greatest effects. Although this conclusion was not reached in our previous study, this was in part explained by the fact the hydrolysis studies were carried out in DMSO and, hence, resulted in much slower hydrolysis rate. Although the assay conditions for studies with T98G cells are different than those used for studies with *T. cruzi*, the latter assays were also carried out in an aqueous culture medium and, hence, the complex would hydrolyze faster than in DMSO. However, the studies carried out here, were performed at a lower concentration than previously used, which increased the hydrolysis rate in the current studies. Studies such as those presented in this work provide guidelines for further investigations seeking to improve potential agents for medicinal applications.

The binding of L^1 to $V(V)$ drastically slowed down its hydrolysis in neutral aqueous solutions, thus, altering the mixed complex's activity spectrum from that of the free ligands. The activity of the simple coordination complex $[V(O)_2(L^1H)]$ can be efficiently regulated by the presence of labile Fe(III), which bound the ligand when released from the complex. Hence, the presence of other metal ions modifies the distribution and activity spectrum of the complexes in both systems. Specificity of some of the known roles of Fe metabolism in cancer and host-pathogen interactions may be in effect (Martínez-Flórez et al., 2020; Dorosti et al., 2014; Perez et al., 2008). This effect is particularly relevant, since for the complexes under consideration L^1H_2 is a known Fe(III) chelating agent and oncogene transformation have been reversed with iron chelation in androgen insensitive prostate cancer and cancer stem cells (Abdelaal and Veuger, 2021). Literature describes various roles

of Fe(III) chelators including inhibition of signaling pathways that drive proliferation, stimulate apoptotic and ER stress signaling pathways, sensitize cancer cells to PARP inhibitors and attenuate oxidative phosphorylation and glycolysis (Yu et al., 2012; Kontoghiorghes, 2022). These are processes which can be utilized in cancer therapy, and reverse oncogenic transformation in the presence of Fe(III) (Abdelaal and Veuger, 2021; Szymonik et al., 2021).

The experimental data shown in Table 1 and Figure 4E demonstrate that $[V(O)_2(L^1H)]$ can be active against human cancer cells at sub-micromolar concentrations, as long as the Fe(III) present in the system is tightly protein-bound. Effective inactivation of $[V(O)_2(L^1H)]$ by serum albumin (Table 1; Figure 4E) showed that the complex can be used for direct injections into tumors (Levina et al., 2020; Levina et al., 2022), but that the complex will be most effective in tumors that are low in albumin and Fe(III) concentrations. Furthermore, such inactivation suggests that the complex that escapes into the blood stream and will then be rapidly inactivated by albumin and not show significant toxicity (Levina et al., 2020; Levina et al., 2022). Similar conclusions can be reached for previous studies with *T. cruzi* trypomastigotes (Scalese et al., 2021). In contrast, the activation by apo-Tf, which is opposite to that observed for other vanadium complexes (Levina and Lay, 2020; Levina et al., 2023), can be explained by Tf chelation of the vanadium to accelerate the release of the Fe chelating ligands. These ligands, in turn, are known to have anti-proliferative activities by interfering with Fe metabolism in the cancer cells.

5 Conclusion

These studies have demonstrated the anti-proliferative activity of the intact and decomposition products of a mixed-ligand $V(V)$ complex, $[VOL^1L^2]$, on human glioblastoma cancer cells. The intact mixed-ligand $V(V)$ complex is known for its anti-trypansomal activity reported previously (Scalese et al., 2021). These studies were done to investigate if a compound exhibiting potent effects as an anti-trypansomal agent also will have activity as an anti cancer agent. In these studies L^1H_2 is Iron Chelator 311 (or NIH, CAS 796-42-9) and L^2 is 5-chloro-7-iodo-8-hydroxyquinoline, also referred to as clioquinol. Speciation studies in aqueous assay solutions are important (Crans et al., 2013; Levina et al., 2017; Levina and Lay, 2017; Nunes et al., 2021; Levina et al., 2023), even when the complex may have limited solubility, or is insoluble in an aqueous assay solution. In the latter cases studies are done in a mixture of organic-aqueous solvents at mM concentration and in aqueous solution at lower concentration. The latter are done using methods that may not be as quantitative as ^{51}V NMR spectroscopy such as UV-vis-NIR and ESI-MS spectroscopy. This work has led to the demonstration of the potent anti-proliferative activities of the intact mixed-ligand $V(V)$ complex ($[V(O) L^1L^2]$), the free ligand (L^1H_2 L^2H) and the precursor complex ($[V(O)_2(L^1H)]$). These data showed that free ligands and the precursor complex were more efficacious than the mixed-ligand $V(V)$ ternary complex ($[V(O) L^1L^2]$) against human glioblastoma cancer cells.

Data availability statement

The original contributions presented in the study are included in the article, further inquiries can be directed to the corresponding authors.

Ethics statement

Ethical approval was not required for the studies on human cell lines in accordance with the local legislation and institutional requirements because only commercially available established cell lines were used.

Author contributions

AL: Conceptualization, Methodology, Project administration, Writing–review and editing, Data curation, Formal Analysis, Investigation, Validation, Writing–original draft. GS: Conceptualization, Data curation, Formal Analysis, Investigation, Methodology, Writing–original draft, Writing–review and editing, Funding acquisition. DG: Conceptualization, Funding acquisition, Methodology, Writing–review and editing, Project administration, Resources, Supervision. DC: Conceptualization, Funding acquisition, Methodology, Project administration, Resources, Supervision, Writing–review and editing. PL: Conceptualization, Funding acquisition, Methodology, Project administration, Resources, Supervision, Writing–review and editing.

Funding

The author(s) declare that financial support was received for the research, authorship, and/or publication of this article. Financial support for this work was provided by Australian Research Council (ARC) Discovery grant to PL for an ARC Senior Research Associate position for AL (DP160104172). DC thanks the Colorado State

University and the Arthur Cope Foundation for partial support. DC and PL thank the University of Sydney for an International Scholar Award to DC. GS and DG thank PEDECIBA and CSIC-UdelaR.

Acknowledgments

The authors thank the Colorado State University Analytical Resources Core Facility, RRID:SCR_021758 for instrument access for the characterization of the compounds and a specific thank you to Dr. Michele Mailhot for assistance with the NMR studies. The authors acknowledge the facilities and the scientific and technical assistance of the Australian Microscopy and Microanalysis Research Facility at the Australian Centre for Microscopy and Microanalysis at the University of Sydney (Drs Minh Huynh and Ellie Kable) for the use of cell culture laboratory. We thank Dr Nicholas Proschogo (Chemistry Mass Spectrometry Facility, the University of Sydney) for performing ICP-MS measurements.

Conflict of interest

The authors declare that the research was conducted in the absence of any commercial or financial relationships that could be construed as a potential conflict of interest.

DC declared that she was an editorial board member of *Frontiers*, at the time of submission. This had no impact on the peer review process and the final decision.

Publisher's note

All claims expressed in this article are solely those of the authors and do not necessarily represent those of their affiliated organizations, or those of the publisher, the editors and the reviewers. Any product that may be evaluated in this article, or claim that may be made by its manufacturer, is not guaranteed or endorsed by the publisher.

References

- Abdelal, G., and Veuger, S. (2021). Reversing oncogenic transformation with iron chelation. *Oncotarget* 12, 106–124. doi:10.18632/oncotarget.27866
- Aureliano, M., De Sousa-Coelho, A. L., Dolan, C. C., Roess, D. A., and Crans, D. C. (2023). Biological consequences of vanadium effects on formation of reactive oxygen species and lipid peroxidation. *Int. J. Mol. Sci.* 24, 5382. doi:10.3390/ijms24065382
- Aureliano, M., Gumerova, N. I., Sciortino, G., Garriba, E., Rompel, A., and Crans, D. C. (2021). Polyoxovanadates with emerging biomedical activities. *Coord. Chem. Rev.* 447, 214143. doi:10.1016/j.ccr.2021.214143
- Bergeron, A., Kostenkova, K., Selman, M., Murakami, H. A., Owens, E., Haribabu, N., et al. (2019). Enhancement of oncolytic virotherapy by vanadium(V) diphosphonates. *BioMetals* 32, 545–561. doi:10.1007/s10534-019-00200-9
- Bijelic, A., Aureliano, M., and Rompel, A. (2019). Polyoxometalates as potential next-generation metallodrugs in the combat against cancer. *Angew. Chem. Int. Ed.* 58, 2980–2999. doi:10.1002/anie.201803868
- Buss, J. L., Arduini, E., and Ponka, P. (2002). Mobilization of intracellular iron by analogs of pyridoxal isonicotinoyl hydrazone (PIH) is determined by the membrane permeability of the iron-chelator complexes. *Biochem. Pharmacol.* 64, 1689–1701. doi:10.1016/s0006-2952(02)01426-0
- Buss, J. L., Arduini, E., Shephard, K. C., and Ponka, P. (2003). Lipophilicity of analogs of pyridoxal isonicotinoyl hydrazone (PIH) determines the efflux of iron complexes and toxicity in K562 cells. *Biochem. Pharmacol.* 65, 349–360. doi:10.1016/s0006-2952(02)01551-4
- Buss, J. L., and Ponka, P. (2003). Hydrolysis of pyridoxal isonicotinoyl hydrazone and its analogs. *Biochimica Biophysica Acta (BBA) - General Subj.* 1619, 177–186. doi:10.1016/s0304-4165(02)00478-6
- Cayman Chemicals (2023). *Clioquinol (item. No. 10021). Product information.* Available at: <https://cdn.caymanchem.com/cdn/insert/10021.pdf> (Accessed December 13, 2023).
- Chauhan, M. S. S., Umar, T., and Aulakh, M. K. (2023). Quinolines: privileged scaffolds for developing new anti-neurodegenerative agents. *ChemistrySelect* 8, e202204960. doi:10.1002/slct.202204960
- Crans, D. C., Henry, L., Cardiff, G., and Posner, B. I. (2019a). Developing vanadium as an antidiabetic or anticancer drug: a clinical and historical perspective. *Mater. Ions Life Sci.* 19, 203–230. doi:10.1515/9783110527872-014
- Crans, D. C., Koehn, J. T., Petry, S. M., Glover, C. M., Wijetunga, A., Kaur, R., et al. (2019b). Hydrophobicity may enhance membrane affinity and anti-cancer effects of Schiff base vanadium(V) catechol complexes. *Dalton Trans.* 48, 6383–6395. doi:10.1039/C9DT00601J
- Crans, D. C., Woll, K. A., Prusinskas, K., Johnson, M. D., and Norkus, E. (2013). Metal speciation in health and medicine represented by iron and vanadium. *Inorg. Chem.* 52, 12262–12275. doi:10.1021/ic4007873

- Debebe, Z., Ammosova, T., Jerebtsova, M., Kurantsin-Mills, J., Niu, X., Charles, S., et al. (2007). Iron chelators ICL670 and 311 inhibit HIV-1 transcription. *Virology* 367, 324–333. doi:10.1016/j.virol.2007.06.011
- Dorosti, Z., Yousefi, M., Sharafi, S. M., and Darani, H. Y. (2014). Mutual action of anticancer and antiparasitic drugs: are there any shared targets? *Future Oncol.* 10, 2529–2539. doi:10.2217/fon.14.65
- Fakhoury, M. (2016). Drug delivery approaches for the treatment of glioblastoma multiforme. *Artif. Cells, Nanomedicine, Biotechnol.* 44, 1365–1373. doi:10.3109/21691401.2015.1052467
- Freshney, R. I. (2016). *Culture of animal cells: a manual of basic technique and specialized applications*. 7th edition. Hoboken, NJ, USA: Wiley-Blackwell.
- Gambino, D. (2011). Potentiality of vanadium compounds as anti-parasitic agents. *Coord. Chem. Rev.* 255, 2193–2203. doi:10.1016/j.ccr.2010.12.028
- Green, D. A., Antholine, W. E., Wong, S. J., Richardson, D. R., and Chitambar, C. R. (2001). Inhibition of malignant cell growth by 311, a novel iron chelator of the pyridoxal isonicotinoyl hydrazone class: effect on the R2 subunit of ribonucleotide reductase. *Clin. Cancer Res.* 7, 3574–3579.
- Griffin, E., Levina, A., and Lay, P. A. (2019). Vanadium(V) tris-3,5-di-tert-butylcatecholato complex: links between speciation and anti-proliferative activity in human pancreatic cancer cells. *J. Inorg. Biochem.* 201, 110815. doi:10.1016/j.jinorgbio.2019.110815
- Hamid, O., Ismail, R., and Puzanov, I. (2020). Intratumoral immunotherapy-update 2019. *Oncol.* 25, e423–e438. doi:10.1634/theoncologist.2019-0438
- Hamidi, A., Hassani, L., Mohammadi, F., Jahangoshayi, P., and Mohammadi, K. (2016). The biological effects of vanadyl curcumin and vanadyl diacetylcurcumin complexes: the effect on structure, function and oxidative stability of the peroxidase enzyme, antibacterial activity and cytotoxic effect. *J. Enzyme Inhibition Med. Chem.* 31, 1124–1131. doi:10.3109/14756366.2015.1101091
- Horton, D. C., Vanderveer, D., Krzystek, J., Telser, J., Pittman, T., Crans, D. C., et al. (2014). Spectroscopic characterization of L-ascorbic acid-induced reduction of vanadium(V) dipicolinate: formation of vanadium(III) and vanadium(IV) complexes from vanadium(V) dipicolinate derivatives. *Inorganica Chim. Acta* 420, 112–119. doi:10.1016/j.ica.2013.12.001
- Ilieva, Y., Dimitrova, L., Zaharieva, M. M., Kaleva, M., Alov, P., Tsakovska, I., et al. (2021). Cytotoxicity and antimicrobial activity of commonly used organic solvents: a comparative study and application to a standardized extract from *Vaccinium macrocarpon*. *Toxics* 9, 92. doi:10.3390/toxics9050092
- Jensen, M. P., Gorman-Lewis, D., Aryal, B., Paunesku, T., Vogt, S., Rickert, P. G., et al. (2011). An iron-dependent and transferrin-mediated cellular uptake pathway for plutonium. *Nat. Chem. Biol.* 7, 560–565. doi:10.1038/nchembio.594
- Joaquim, A. R., Gionbelli, M. P., Gosmann, G., Fuentesfria, A. M., Lopes, M. S., and Fernandes De Andrade, S. (2021). Novel antimicrobial 8-hydroxyquinoline-based agents: current development, structure-activity relationships, and perspectives. *J. Med. Chem.* 64, 16349–16379. doi:10.1021/acs.jmedchem.1c01318
- John, S. F., Aniemeke, E., Ha, N. P., Chong, C. R., Gu, P., Zhou, J., et al. (2016). Characterization of 2-hydroxy-1-naphthaldehyde isonicotinoyl hydrazone as a novel inhibitor of methionine aminopeptidases from *Mycobacterium tuberculosis*. *Tuberculosis* 101, S73–S77. doi:10.1016/j.tube.2016.09.025
- Kalinowski, D. S., Sharpe, P. C., Bernhardt, P. V., and Richardson, D. R. (2008). Structure-activity relationships of novel iron chelators for the treatment of iron overload disease: the methyl pyrazinylketone isonicotinoyl hydrazone series. *J. Med. Chem.* 51, 331–344. doi:10.1021/jm7012562
- Khan, R., Khan, H., Abdullah, Y., and Dou, Q. P. (2020). Feasibility of repurposing clioquinol for cancer therapy. *Recent Pat. Anti-Cancer Drug Discov.* 15, 14–31. doi:10.2174/1574892815666200227090259
- Kinnamon, K. E., Steck, E. A., and Rane, D. S. (1979). Activity of antitumor drugs against African trypanosomes. *Antimicrob. Agents Chemother.* 15, 157–160. doi:10.1128/aac.15.2.157
- Kontoghiorghes, G. J. (2022). New iron metabolic pathways and chelation targeting strategies affecting the treatment of all types and stages of cancer. *Int. J. Mol. Sci.* 23, 13990. doi:10.3390/ijms232213990
- Kostenkova, K., Althumairy, D., Rajan, A., Kortz, U., Barisas, B. G., Roess, D. A., et al. (2023a). Polyoxidoanadates $[\text{Mo}^{\text{VI}}\text{V}^{\text{V}}_9\text{O}_{28}]^{2-}$ and $[\text{H}_2\text{Pt}^{\text{IV}}\text{V}^{\text{V}}_9\text{O}_{28}]^{3-}$ interact with CHO cell plasma membrane lipids causing aggregation and activation of a G protein-coupled receptor. *Front. Chem. Biol.* 2. doi:10.3389/fchbi.2023.1126975
- Kostenkova, K., Levina, A., Walters, D. A., Murakami, H. A., Lay, P. A., and Crans, D. C. (2023b). Vanadium(V) pyridine-containing Schiff base catecholates complexes are lipophilic, redox-active and selectively cytotoxic in glioblastoma (T98G) cells. *Chem. Eur. J.* 29, e202302271. doi:10.1002/chem.202302271
- Kostenkova, K., Klugh, K., and Crans, D. C. (2024). “Recent advances of medicinal properties of vanadium compounds: cancer and other diseases,” in *Metal ions in life sciences*, Chap. 2, Ana de Bettencourt-Dias.
- Kowalski, S., Wyrzykowski, D., and Inkielewicz-Stepniak, I. (2020). Molecular and cellular mechanisms of cytotoxic activity of vanadium compounds against cancer cells. *Molecules* 25, 1757. doi:10.3390/molecules25071757
- Lanza, V., Milardi, D., Di Natale, G., and Pappalardo, G. (2018). Repurposing of copper(II)-chelating drugs for the treatment of neurodegenerative diseases. *Curr. Med. Chem.* 25, 525–539. doi:10.2174/0929867324666170518094404
- Le, M., Rathje, O., Levina, A., and Lay, P. A. (2017). High cytotoxicity of vanadium(IV) complexes with 1,10-phenanthroline and related ligands is due to decomposition in cell culture medium. *J. Biol. Inorg. Chem.* 22, 663–672. doi:10.1007/s00775-017-1453-4
- Levina, A., Crans, D. C., and Lay, P. A. (2017). Speciation of metal drugs, supplements and toxins in media and bodily fluids controls *in vitro* activities. *Coord. Chem. Rev.* 352, 473–498. doi:10.1016/j.ccr.2017.01.002
- Levina, A., Crans, D. C., and Lay, P. A. (2022). Advantageous reactivity of unstable metal complexes: potential applications of metal-based anticancer drugs for intratumoral injections. *Pharmaceutics* 14, 790. doi:10.3390/pharmaceutics14040790
- Levina, A., and Lay, P. A. (2011). Metal-based anti-diabetic drugs: advances and challenges. *Dalton Trans.* 40, 11675–11686. doi:10.1039/C1DT10380F
- Levina, A., and Lay, P. A. (2017). Stabilities and biological activities of vanadium drugs: what is the nature of the active species? *Chem. - Asian J.* 12, 1692–1699. doi:10.1002/asia.201700463
- Levina, A., and Lay, P. A. (2020). Vanadium(V/IV)-transferrin binding disrupts the transferrin cycle and reduces vanadium uptake and antiproliferative activity in human lung cancer cells. *Inorg. Chem.* 59, 16143–16153. doi:10.1021/acs.inorgchem.0c00926
- Levina, A., Pires Vieira, A., Wijetunga, A., Kaur, R., Koehn, J. T., Crans, D. C., et al. (2020). A short-lived but highly cytotoxic vanadium(V) complex as a potential drug lead for brain cancer treatment by intratumoral injections. *Angew. Chem. Int. Ed.* 59, 15834–15838. doi:10.1002/anie.202005458
- Levina, A., Usulan, C., Murakami, H., Crans, D. C., and Lay, P. A. (2023). Substitution kinetics, albumin and transferrin affinities, and hypoxia all affect the biological activities of anticancer vanadium(V) complexes. *Inorg. Chem.* 62, 17804–17817. doi:10.1021/acs.inorgchem.3c02561
- Lopez, J., Ramchandani, D., and Vahdat, L. (2019). Copper depletion as a therapeutic strategy in cancer. *Metal ions life Sci.* 19, 303–330. doi:10.1515/9783110527872-018
- Machado, J. F., Marques, F., Pinheiro, T., Villa de Brito, M. J., Scalse, G., Pérez-Díaz, L., et al. (2023). Copper(I)-thiosemicarbazone complexes with dual anticancer and antiparasitic activity. *ChemMedChem* 18, e202300074. doi:10.1002/cmdc.202300074
- Martínez-Flórez, A., Galizzi, M., Izquierdo, L., Bustamante, J. M., Rodríguez, A., Rodríguez, F., et al. (2020). Repurposing bioenergetic modulators against protozoan parasites responsible for tropical diseases. *Int. J. Parasitol. Drugs Drug Resist.* 14, 17–27. doi:10.1016/j.ijpddr.2020.07.002
- McAusland, T. M., van Vloten, J. P., Santry, L. A., Guilleman, M. M., Rghei, A. D., Ferreira, E. M., et al. (2021). Combining vanadyl sulfate with Newcastle disease virus potentiates rapid innate immune-mediated regression with curative potential in murine cancer models. *Mol. Ther. - Oncolytics* 20, 306–324. doi:10.1016/j.omto.2021.01.009
- Melnik, P., Leroux, V., Sergheraert, C., and Grellier, P. (2006). Design, synthesis and *in vitro* antimalarial activity of an acylhydrazone library. *Bioorg. Med. Chem. Lett.* 16, 31–35. doi:10.1016/j.bml.2005.09.058
- Mosquillo, M. F., Smircich, P., Lima, A., Gehrke, S. A., Scalse, G., Machado, I., et al. (2020). High throughput approaches to unravel the mechanism of action of a new vanadium-based compound against *Trypanosoma cruzi*. *Bioinorganic Chem. Appl.* 2020, 1–10. doi:10.1155/2020/1634270
- Murakami, H. A., Usulan, C., Haase, A. A., Koehn, J. T., Vieira, A. P., Gaebler, D. J., et al. (2022). Vanadium chloro-substituted Schiff base catecholates complexes are reducible, lipophilic, water stable, and have anticancer activities. *Inorg. Chem.* 61, 20757–20773. doi:10.1021/acs.inorgchem.2c02557
- Nunes, P., Correia, I., Cavaco, I., Marques, F., Pinheiro, T., Aveçilla, F., et al. (2021). Therapeutic potential of vanadium complexes with 1,10-phenanthroline ligands, *quo vadis?* Fate of complexes in cell media and cancer cells. *J. Inorg. Biochem.* 217, 111350. doi:10.1016/j.jinorgbio.2020.111350
- Odularu, A. T., Ajibade, P. A., Mbese, J. Z., and Oyedeji, O. O. (2019). Developments in platinum-group metals as dual antibacterial and anticancer agents. *J. Chem.* 2019, 5459461–5459518. doi:10.1155/2019/5459461
- Oliveri, V., and Vecchio, G. (2016). 8-Hydroxyquinolines in medicinal chemistry: a structural perspective. *Eur. J. Med. Chem.* 120, 252–274. doi:10.1016/j.ejmech.2016.05.007
- Perez, D. R., Sklar, L. A., and Chigaev, A. (2019). Clioquinol: to harm or heal. *Pharmacol. Ther.* 199, 155–163. doi:10.1016/j.pharmthera.2019.03.009
- Perez, J., Fuertes, M., Nguewa, P., Castilla, J., and Alonso, C. (2008). Anticancer compounds as leishmanicidal drugs: challenges in chemotherapy and future perspectives. *Curr. Med. Chem.* 15, 433–439. doi:10.2174/092986708783503221
- Pessoa, J. C., Etcheverry, S., and Gambino, D. (2015). Vanadium compounds in medicine. *Coord. Chem. Rev.* 301–302, 24–48. doi:10.1016/j.ccr.2014.12.002
- Pisano, M., Arru, C., Serra, M., Galleri, G., Sanna, D., Garriba, E., et al. (2019). Antiproliferative activity of vanadium compounds: effects on the major malignant melanoma molecular pathways. *Metallomics* 11, 1687–1699. doi:10.1039/c9mt00174c
- Prachayasittikul, V., Prachayasittikul, S., Ruchirawat, S., and Prachayasittikul, V. (2013). 8-Hydroxyquinolines: a review of their metal chelating properties and medicinal applications. *Drug Des. Dev. Ther.* 7, 1157–1178. doi:10.2147/DDDT.S49763

- Przybyło, M., and Langner, M. (2020). On the physiological and cellular homeostasis of ascorbate. *Cell. Mol. Biol. Lett.* 25, 32. doi:10.1186/s11658-020-00223-y
- Reytman, L., Hochman, J., and Tshuva, E. Y. (2018). Anticancer diaminotris(phenolato) vanadium(V) complexes: ligand-metal interplay. *J. Coord. Chem.* 71, 2003–2011. doi:10.1080/00958972.2018.1461848
- Richardson, D. R., and Bernhardt, P. V. (1999). Crystal and molecular structure of 2-hydroxy-1-naphthaldehyde isonicotinoyl hydrazone (NIH) and its iron(III) complex: an iron chelator with anti-tumour activity. *J. Biol. Inorg. Chem.* 4, 266–273. doi:10.1007/s007750050312
- Richardson, D. R., Tran, E. H., and Ponka, P. (1995). The potential of iron chelators of the pyridoxal isonicotinoyl hydrazone class as effective antiproliferative agents. *Blood* 86, 4295–4306. doi:10.1182/blood.v86.11.4295.bloodjournal86114295
- Ritchie, R. F., Palomaki, G. E., Neveux, L. M., Navolotskaia, O., Ledue, T. B., and Craig, W. Y. (2002). Reference distributions for serum iron and transferrin saturation: a practical, simple, and clinically relevant approach in a large cohort. *J. Clin. Laboratory Analysis* 16, 237–245. doi:10.1002/jcla.10048
- Rivas, F., Medeiros, A., Comini, M., Suescun, L., Rodríguez Arce, E., Martins, M., et al. (2019). Pt-Fe ferrocenyl compounds with hydroxyquinoline ligands show selective cytotoxicity on highly proliferative cells. *J. Inorg. Biochem.* 199, 110779. doi:10.1016/j.jinorgbio.2019.110779
- Sah, P. P. T., and Peoples, S. A. (1954). Isonicotinyl hydrazones as antitubercular agents and derivatives for identification of aldehydes and ketones. *J. Am. Pharm. Assoc. Sci. ed.* 43, 513–524. doi:10.1002/jps.3030430902
- Santos, S. S., de Araújo, R. V., Giarolla, J., Seoud, O. E., and Ferreira, E. I. (2020). Searching for drugs for Chagas disease, leishmaniasis and schistosomiasis: a review. *Int. J. Antimicrob. Agents* 55, 105906. doi:10.1016/j.ijantimicag.2020.105906
- Sarmiento-Gonzalez, A., Marchante-Gayon, J. M., Tejerina-Lobo, J. M., Paz-Jimenez, J., and Sanz-Medel, A. (2005). ICP-MS multielemental determination of metals potentially released from dental implants and articular prostheses in human biological fluids. *Anal. Bioanal. Chem.* 382, 1001–1009. doi:10.1007/s00216-005-3165-9
- Scalese, G., Arhouma, Z., Kostenkova, K., Pérez-Díaz, L., Crick, D. C., Gambino, D., et al. (2022a). Do bioactive 8-hydroxyquinolines oxidovanadium(IV) and (V) complexes inhibit the growth of *M. smegmatis*? *J. Inorg. Biochem.* 237, 111984. doi:10.1016/j.jinorgbio.2022.111984
- Scalese, G., Benitez, J., Rostan, S., Correia, I., Bradford, L., Vieites, M., et al. (2015). Expanding the family of heteroleptic oxidovanadium(IV) compounds with salicylaldehyde semicarbazones and polypyridyl ligands showing anti-*Trypanosoma cruzi* activity. *J. Inorg. Biochem.* 147, 116–125. doi:10.1016/j.jinorgbio.2015.03.002
- Scalese, G., Kostenkova, K., Crans, D. C., and Gambino, D. (2022b). Metallomics and other omics approaches in antiparasitic metal-based drug research. *Curr. Opin. Chem. Biol.* 67, 102127. doi:10.1016/j.cbpa.2022.102127
- Scalese, G., Machado, I., Correia, I., Pessoa, J. C., Bilbao, L., Pérez-Díaz, L., et al. (2019). Exploring oxidovanadium(IV) homoleptic complexes with 8-hydroxyquinoline derivatives as prospective antitrypanosomal agents. *New J. Chem.* 43, 17756–17773. doi:10.1039/C9NJ02589H
- Scalese, G., Machado, I., Fontana, C., Risi, G., Salinas, G., Pérez-Díaz, L., et al. (2018). New heteroleptic oxidovanadium(V) complexes: synthesis, characterization and biological evaluation as potential agents against *Trypanosoma cruzi*. *J. Biol. Inorg. Chem.* 23, 1265–1281. doi:10.1007/s00775-018-1613-1
- Scalese, G., Machado, I., Salinas, G., Pérez-Díaz, L., and Gambino, D. (2021). Heteroleptic oxidovanadium(V) complexes with activity against infective and non-infective stages of *Trypanosoma cruzi*. *Molecules* 26, 5375. doi:10.3390/molecules26175375
- Scalese, G., Mosquillo, M. F., Rostan, S., Castiglioni, J., Alho, I., Perez, L., et al. (2017). Heteroleptic oxidovanadium(IV) complexes of 2-hydroxynaphthylaldimine and polypyridyl ligands against *Trypanosoma cruzi* and prostate cancer cells. *J. Inorg. Biochem.* 175, 154–166. doi:10.1016/j.jinorgbio.2017.07.014
- Scior, T., Guevara-Garcia, J., Do, Q.-T., Bernard, P., and Laufer, S. (2016). Why antidiabetic vanadium complexes are not in the pipeline of “big pharma” drug research? A critical review. *Curr. Med. Chem.* 23, 2874–2891. doi:10.2174/0929867323666160321121138
- Selman, M., Rouso, C., Bergeron, A., Son, H. H., Krishnan, R., El-Sayes, N. A., et al. (2018). Multi-modal potentiation of oncolytic virotherapy by vanadium compounds. *Mol. Ther.* 26, 56–69. doi:10.1016/j.ymthe.2017.10.014
- Song, Y., Xu, H., Chen, W., Zhan, P., and Liu, X. (2015). 8-Hydroxyquinoline: a privileged structure with a broad-ranging pharmacological potential. *MedChemComm* 6, 61–74. doi:10.1039/c4md00284a
- Sylvester, P. W. (2011). Optimization of the tetrazolium dye (MTT) colorimetric assay for cellular growth and viability. *Methods Mol. Biol.* 716, 157–168. doi:10.1007/978-1-61779-012-6_9
- Szymonik, J., Wala, K., Górnicki, T., Saczko, J., Pencakowski, B., and Kulbacka, J. (2021). The impact of iron chelators on the biology of cancer stem cells. *Int. J. Mol. Sci.* 23, 89. doi:10.3390/ijms23010089
- Thompson, K. H., Lichter, J., Lebel, C., Scaife, M. C., McNeill, J. H., and Orvig, C. (2009). Vanadium treatment of type 2 diabetes: a view to the future. *J. Inorg. Biochem.* 103, 554–558. doi:10.1016/j.jinorgbio.2008.12.003
- Walcourt, A., Loyevsky, M., Lovejoy, D. B., Gordeuk, V. R., and Richardson, D. R. (2004). Novel aroylhydrazone and thiosemicarbazone iron chelators with anti-malarial activity against chloroquine-resistant and -sensitive parasites. *Int. J. Biochem. Cell Biol.* 36, 401–407. doi:10.1016/s1357-2725(03)00248-6
- Whitnall, M., Howard, J., Ponka, P., and Richardson, D. R. (2006). A class of iron chelators with a wide spectrum of potent antitumor activity that overcomes resistance to chemotherapeutics. *Proc. Natl. Acad. Sci. U. S. A.* 103, 14901–14906. doi:10.1073/pnas.0604979103
- WHO (2023). Chagas disease (also known as American trypanosomiasis). Available at: https://www.who.int/health-topics/chagas-disease#tab=tab_1
- Wilkins, P. C., Johnson, M. D., Holder, A. A., and Crans, D. C. (2006). Reduction of vanadium(V) by L-ascorbic acid at low and neutral pH: kinetic, mechanistic, and spectroscopic characterization. *Inorg. Chem.* 45, 1471–1479. doi:10.1021/ic050749g
- Willisky, G. R., Chi, L.-H., Godzala, M., III, Kostyniak, P. J., Smee, J. J., Trujillo, A. M., et al. (2011). Anti-diabetic effects of a series of vanadium dipicolinate complexes in rats with streptozotocin-induced diabetes. *Coord. Chem. Rev.* 255, 2258–2269. doi:10.1016/j.ccr.2011.06.015
- Wu, D., Chen, Q., Chen, X., Han, F., Chen, Z., and Wang, Y. (2023). The blood–brain barrier: structure, regulation, and drug delivery. *Signal Transduct. Target. Ther.* 8, 217. doi:10.1038/s41392-023-01481-w
- Yu, Y., Gutierrez, E., Kovacevic, Z., Saletta, F., Obeidy, P., Suryo Rahmanto, Y., et al. (2012). Iron chelators for the treatment of cancer. *Curr. Med. Chem.* 19, 2689–2702. doi:10.2174/092986712800609706